

**Microphysical and thermodynamic
retrievals using polarimetric radars
Latest updates**

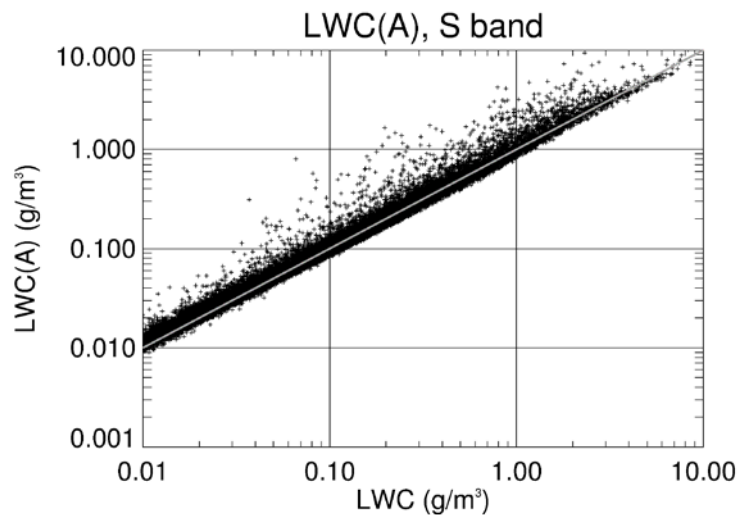
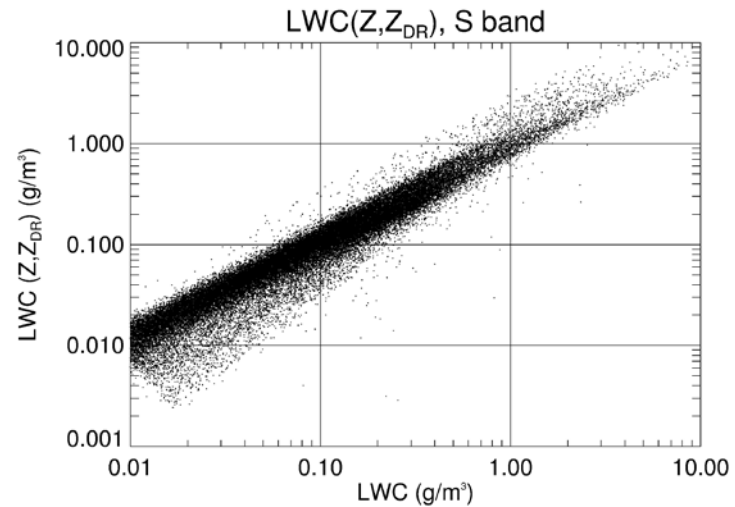
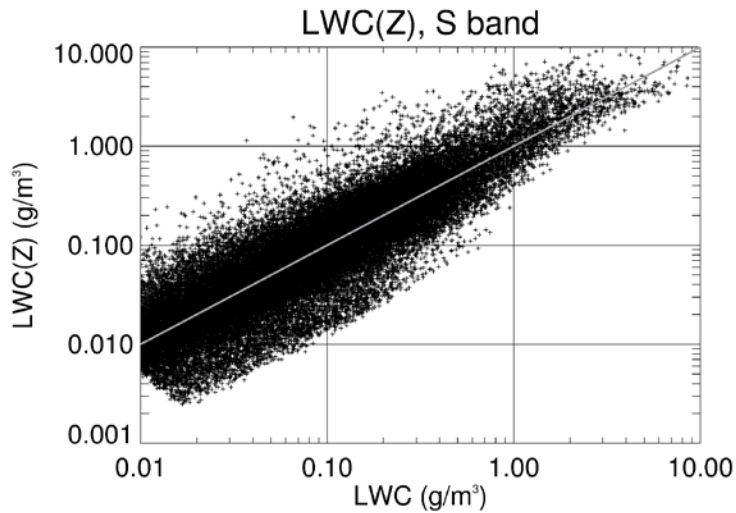
Alexander Ryzhkov

University of Oklahoma, USA

PROM meeting, 23 October 2019

Rain microphysical retrievals

Radar estimates of liquid water content LWC



S band

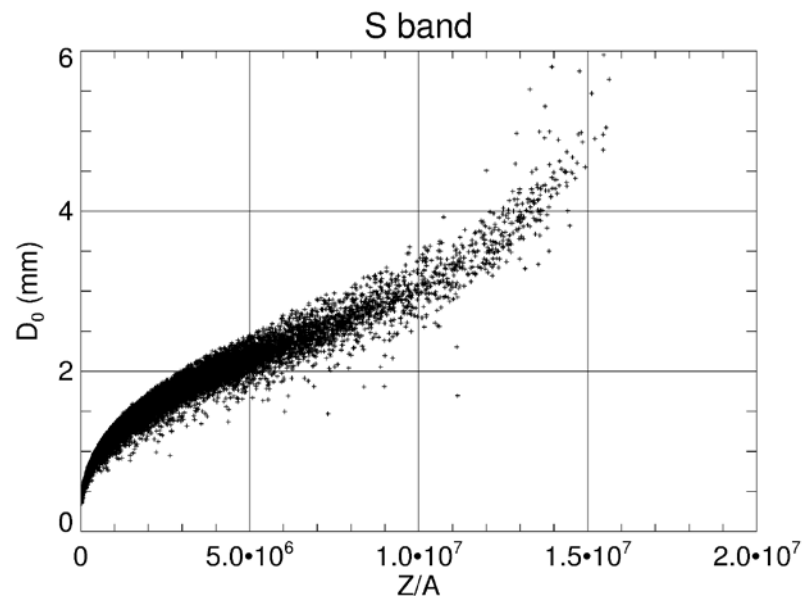
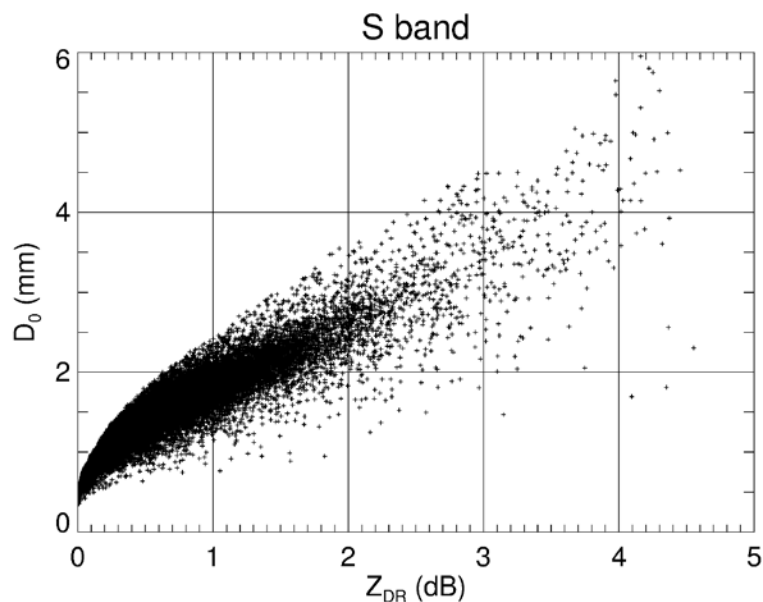
$$LWC(Z) = 1.74 \cdot 10^{-3} Z^{0.64}$$

$$LWC(Z, Z_{DR}) = 1.38 \cdot 10^{-3} Z \cdot 10^{(-2.43Z_{DR} + 1.12Z_{DR}^2 - 0.176Z_{DR}^3)}$$

$$LWC(A) = 115 A^{0.92}$$

$$[Z] = mm^6 m^{-3}, \quad [Z_{DR}] = dB, \quad [A] = dB / km, \quad [LWC] = deg / km$$

Estimation of the mean volume diameter of raindrops D_m



Bringi and Chandrasekar (2001)

$$D_m = 1.62 Z_{DR}^{0.49}$$

S band

$$D_m = 0.630 + 0.675x - 0.124x^2 + 0.0115x^3 - 0.00034x^4$$

Bringi et al. (2002)

$$D_m = 1.97 Z_{DR}^{0.49}$$

$$x = \frac{Z}{A} 10^{-6}$$

$$[Z] = mm^6 m^{-3}, \quad [Z_{DR}] = dB, \quad [A] = dB / km, \quad [D_m] = mm$$

Caveats: Z_{DR} should be well calibrated, A is a function of radar wavelength and temperature

Estimation of total number concentration of raindrops N_t

$$N_t = 20.4 \frac{LWC}{D_m^3}$$

$$[N_t] = 1/L, \quad [LWC] = g/m^3, \quad [D_m] = mm$$

Ice microphysical retrievals

- All existing ice microphysical retrievals are based on the use of radar reflectivity Z measured at a single or multiple radar frequencies
- The $IWC(Z)$ relations are notoriously inaccurate because they are strongly parameterized by (a) mass-weighted diameter D_m , (b) total concentration N_t , and (c) density (or degree of riming)

$$N(D) = N_{0s} \exp(-\Lambda_s D) \quad \rho(D) = \alpha D^{-1} \quad \Lambda_s = 4 / D_m$$

$$IWC = 3.81 10^{-4} \alpha^{-0.2} N_{0s}^{0.4} Z^{0.6} \quad IWC = 3.09 10^{-3} \frac{Z}{\alpha D_m^2}$$

- D_m varies 2 orders of magnitude
- N_t varies 4 orders of magnitude
- α changes at least by a factor of 4

Basic formulas for polarimetric ice retrievals

$$Z = \frac{|K_i|^2}{|K_w|^2} \frac{1}{\rho_i^2} \int \rho_s^2(D) D^6 N(D) dD$$

$$K_{DP} = \frac{0.27\pi}{\lambda \rho_i^2} \left(\frac{\epsilon_i - 1}{\epsilon_i + 2} \right)^2 \int F_{shape} F_{orient} \rho_s^2(D) D^3 N(D) dD$$

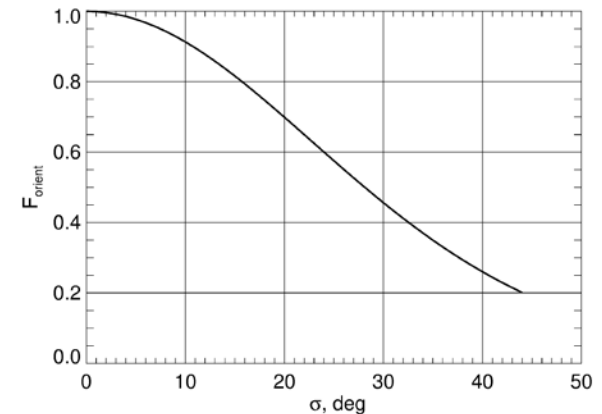
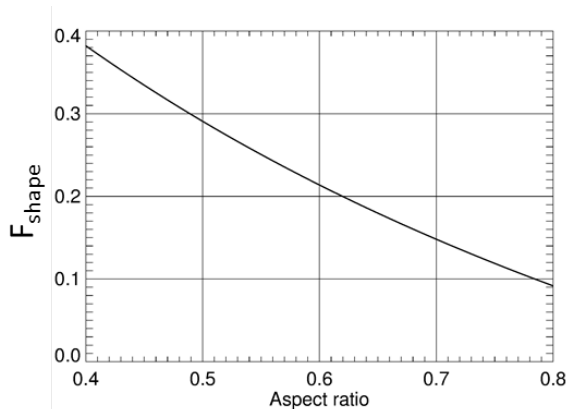
***Z is proportional to the 4th moment of snow SD whereas
K_{DP} is proportional to its 1st moment***

Exponential size distribution

$$Z = 5.30 \cdot 10^{-3} \alpha^2 N_{0s} D_m^5$$

$$K_{DP} = 1.02 \cdot 10^{-2} F_{shape} F_{orient} \frac{\alpha^2 N_{0s}}{\lambda} D_m^2$$

$$\frac{Z}{K_{DP} \lambda} = 0.520 \frac{D_m^3}{F_{shape} F_{orient}}$$



Formulas for ice microphysical retrievals

Ryzhkov and Zrnic “Radar Polarimetry for Weather Observations” (2019)

$$D_m = -0.1 + 2.0 \left(\frac{Z_{DP}}{K_{DP} \lambda} \right)^{1/2}$$

D_m (mm) – mean volume diameter

$$\log(N_t) = 0.1Z(\text{dBZ}) - 2 \log \left(\frac{Z_{DP}}{K_{DP} \lambda} \right) - 1.11$$

N_t (1/L) – total concentration

$$IWC = 4.0 \cdot 10^{-3} \frac{Z}{Z_{DP}} K_{DP} \lambda = 4.0 \cdot 10^{-3} \frac{K_{DP} \lambda}{1 - Z_{dr}^{-1}}$$

IWC (g/m³) – ice water content

$Z_{DP} = Z_h - Z_v$ - reflectivity difference (mm⁶m⁻³)

Z_{dr} - differential reflectivity (linear scale)

K_{DP} – specific differential phase (deg km⁻¹)

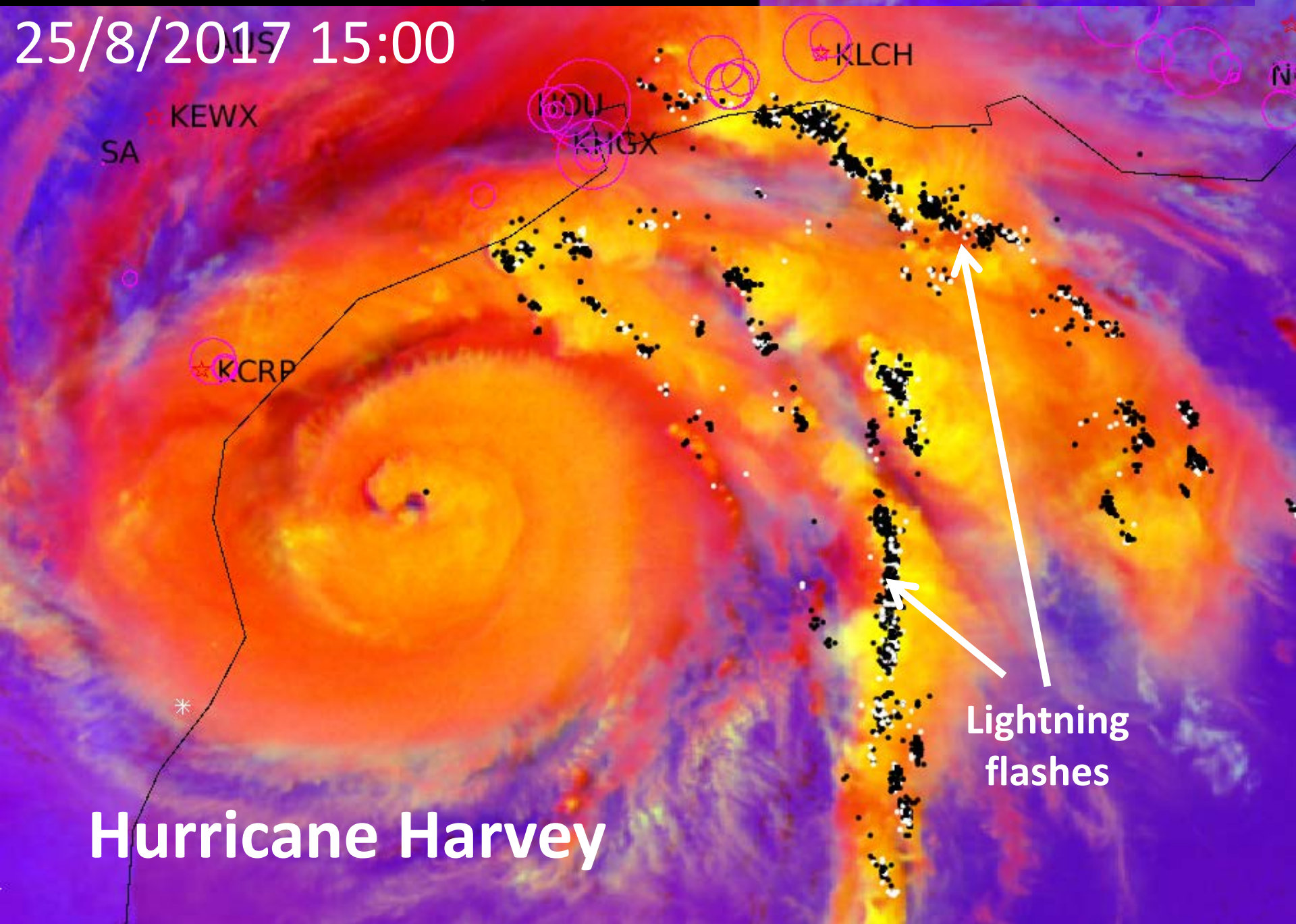
λ – radar wavelength (mm)

- Polarimetric retrieval equations are not valid for non-Rayleigh scatterers and graupel / hail
- The estimates are almost insensitive to the variability of size distributions, shapes, and orientations of ice particles
- They do not work for very low K_{DP} and Z_{DR} (Z_{DP})

The impact of measurements errors of K_{DP} and Z_{DR} (Z_{DP})

- Statistical errors of the point measurements of K_{DP} and Z_{DR} are prohibitively large. $SD(D_m) > 70\%$ if $K_{DP} < 0.05$ deg/km at S band ; $SD(D_m) > 25\%$ if $Z_{DR} < 0.2$ dB. The accuracy improves at shorter wavelengths
- Aggressive spatial averaging of K_{DP} and Z_{DR} is required to obtain their meaningful values which inevitably results in the degradation of spatial resolution
- Various techniques for processing and presentation of polarimetric radar data have been developed recently (QVP, range-defined QVP, CVP, 4D-grid) to reveal polarimetric signatures in ice / snow, to reduce statistical errors in polarimetric radar variables, and improve their vertical resolution
- The best results are achieved in the dendritic growth layer and the worst are just above the freezing level where K_{DP} and Z_{DR} signatures almost vanish as a result of strong aggregation of dry snowflakes

25/8/2017 15:00



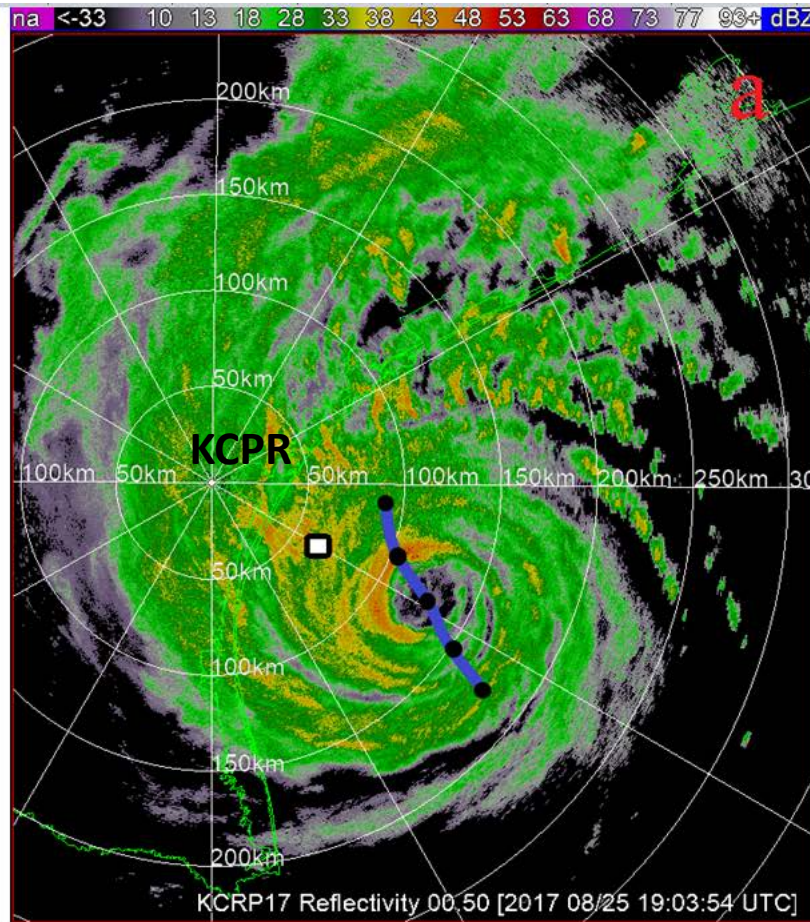
Hurricane Harvey

Lightning
flashes

Hurricane Harvey

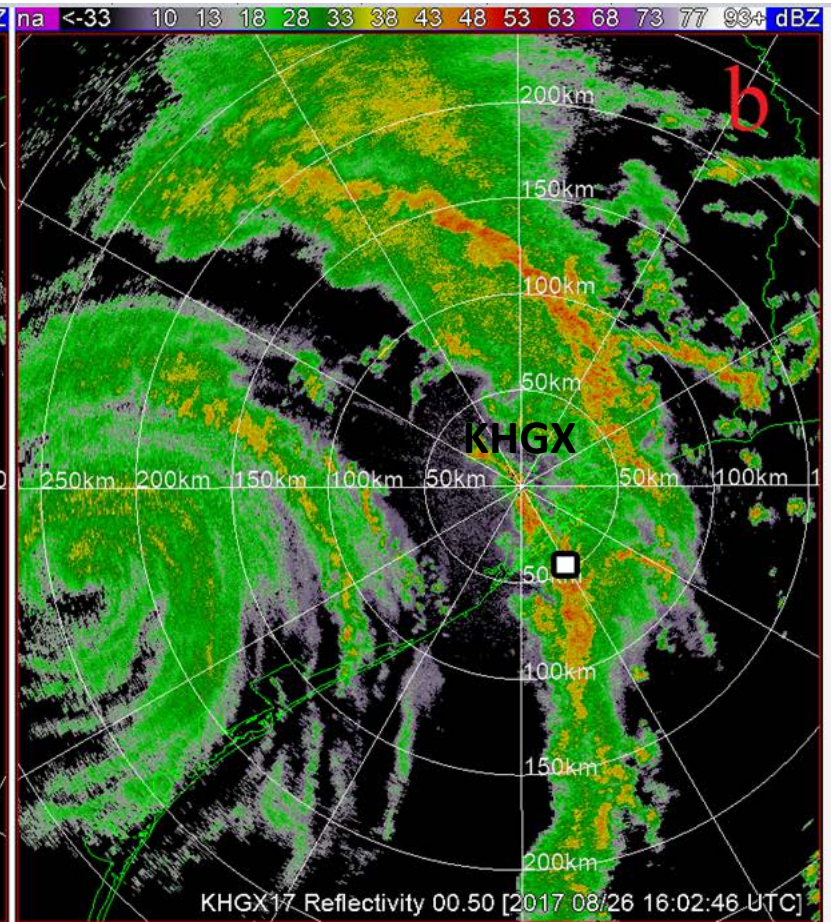
Eyewall

From the perspective of the
KCPR WSR-88D radar



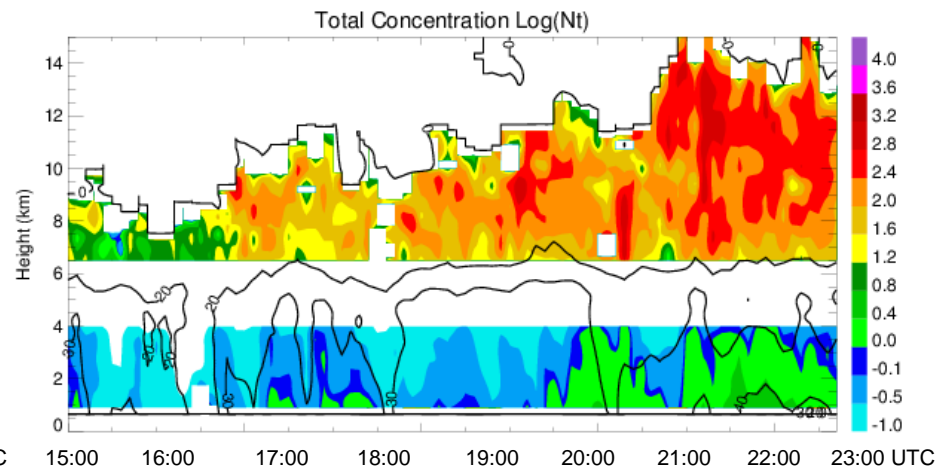
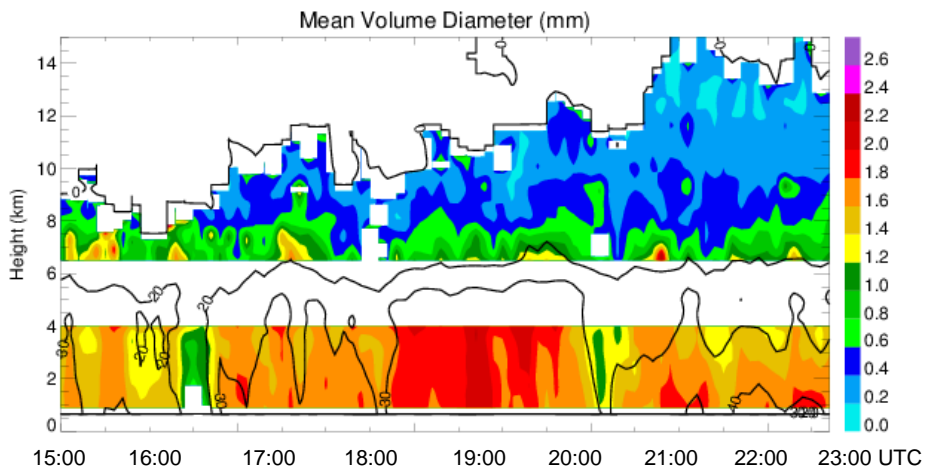
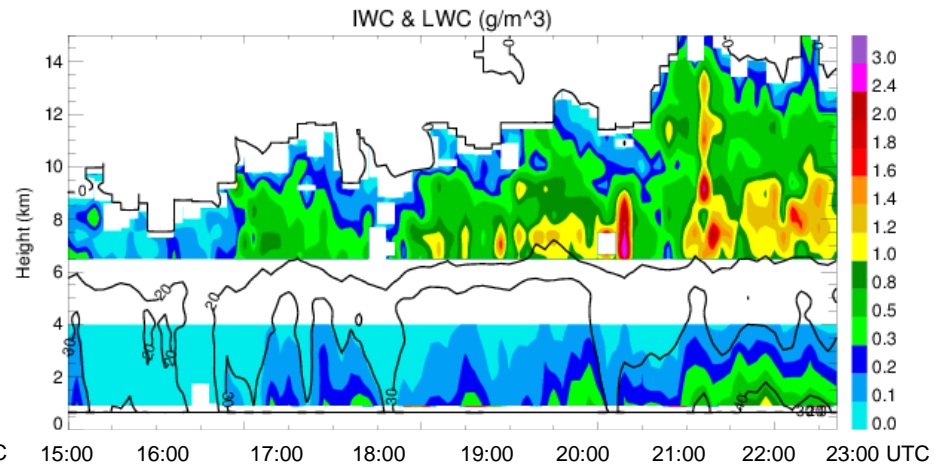
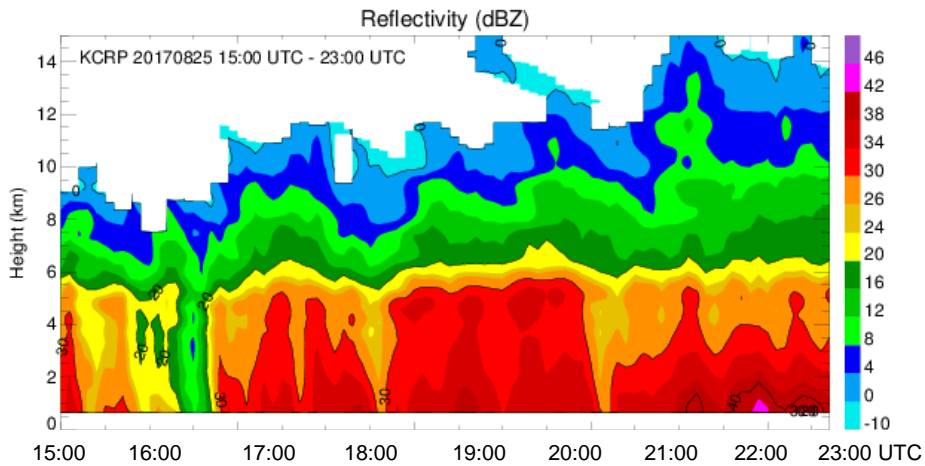
External rain band

From the perspective of the
KHGX WSR-88D radar



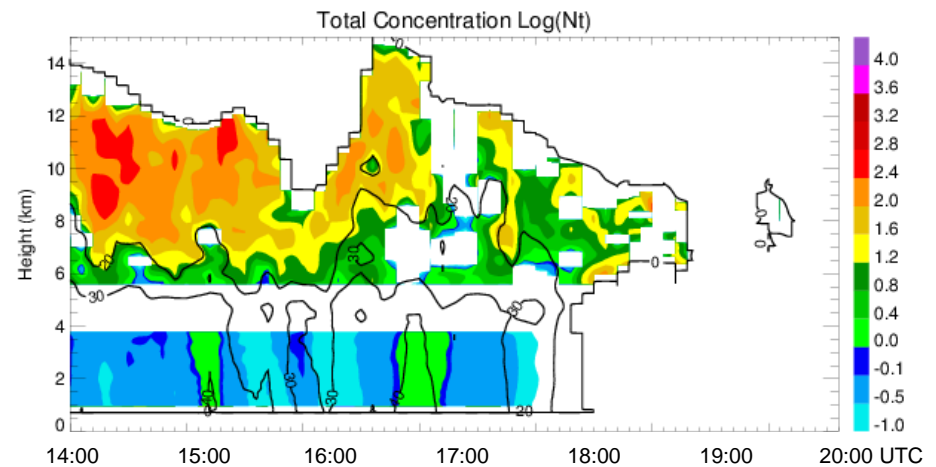
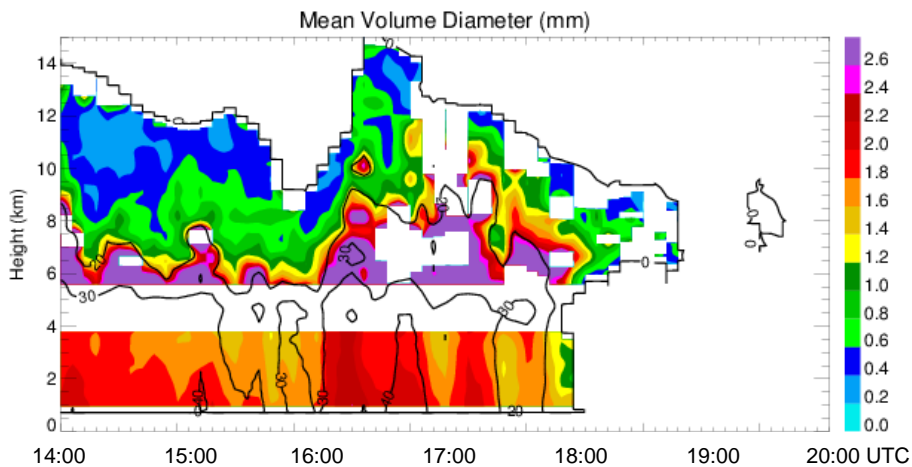
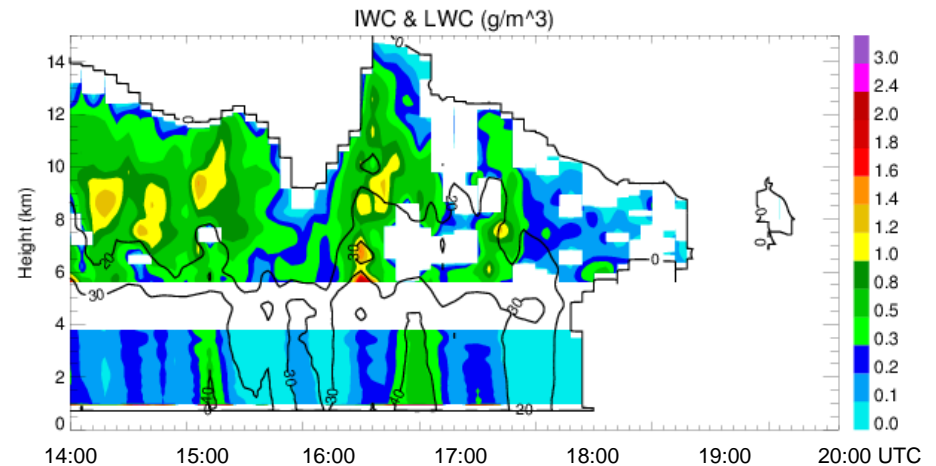
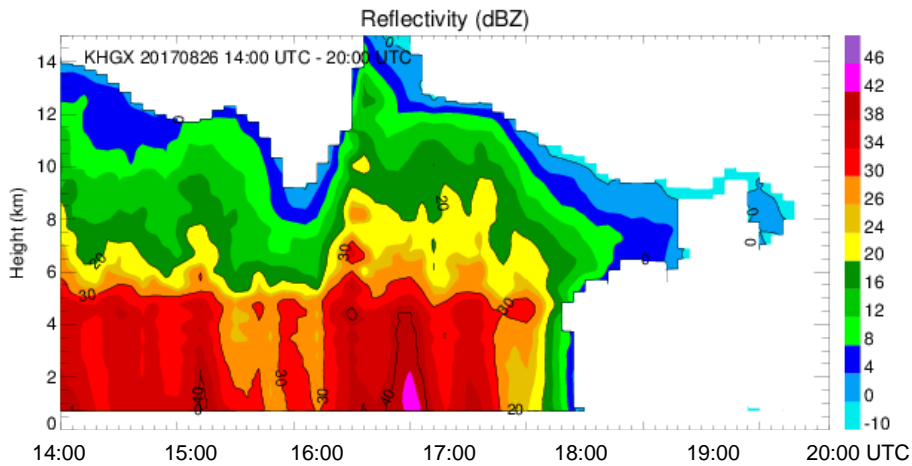
KCRP 20170825

R=60 km, Azm=120°



KHGX 20170826

R=40 km, Azm=130°



Dual-frequency polarimetric radar measurements with Ka-band and S-band radars

Courtesy of Pavlos Kollias and Mariko Oue

KASPR

WSR-88D

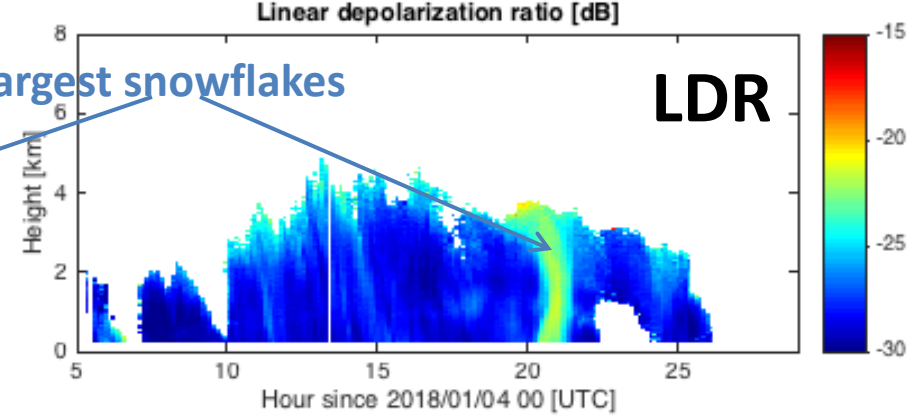
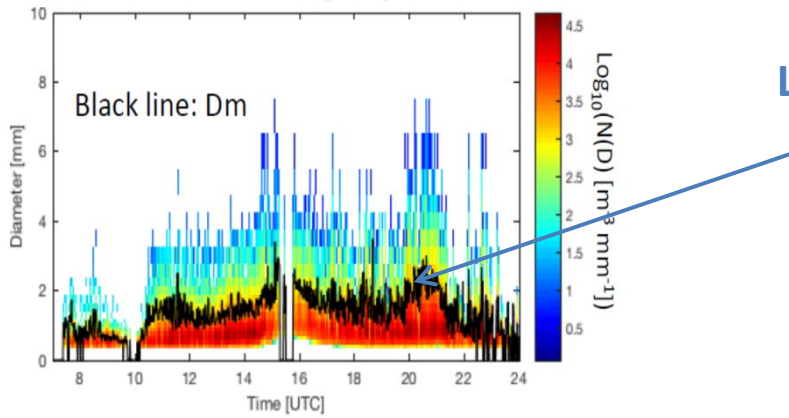
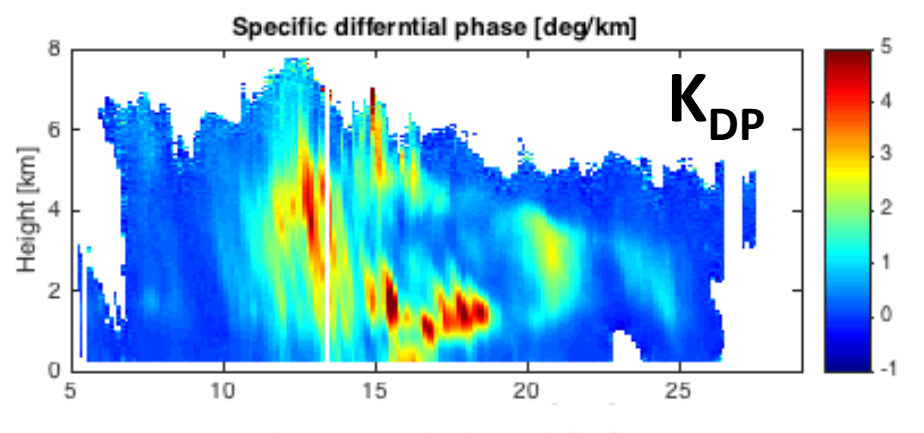
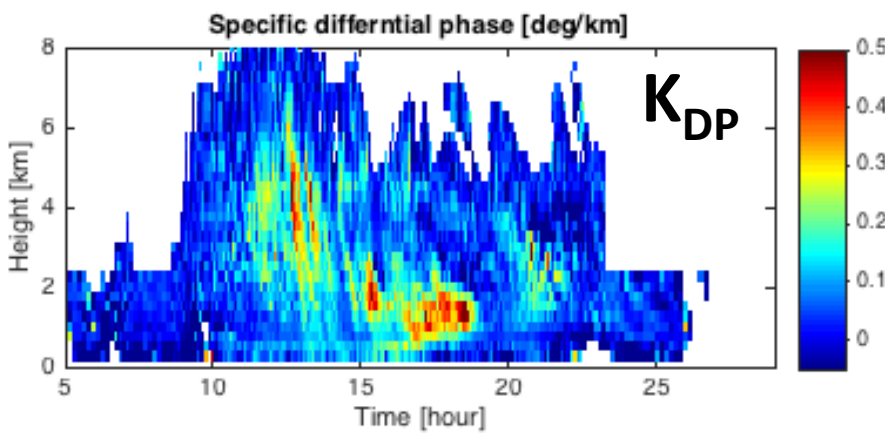
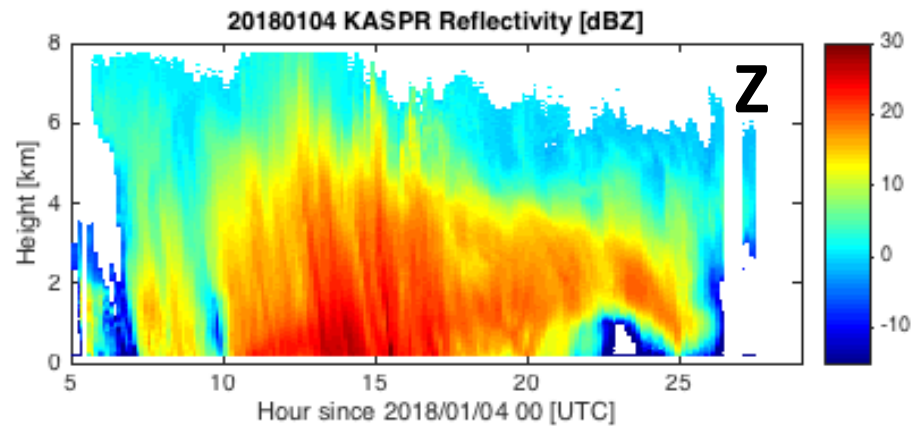
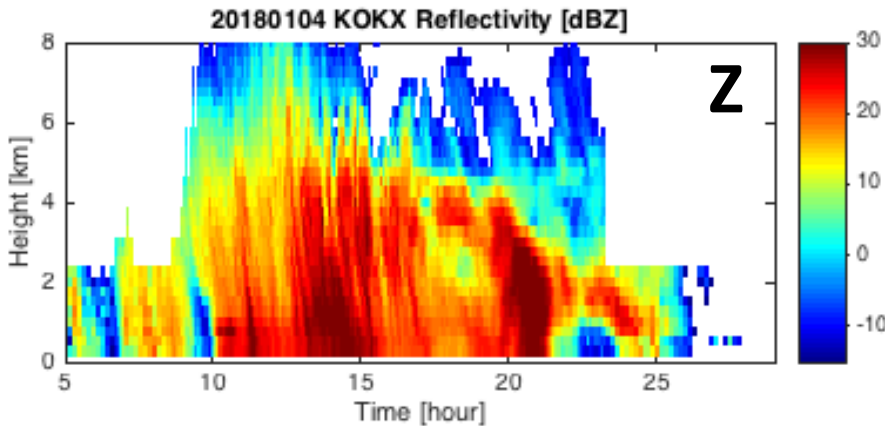


SBU – Stony Brook University

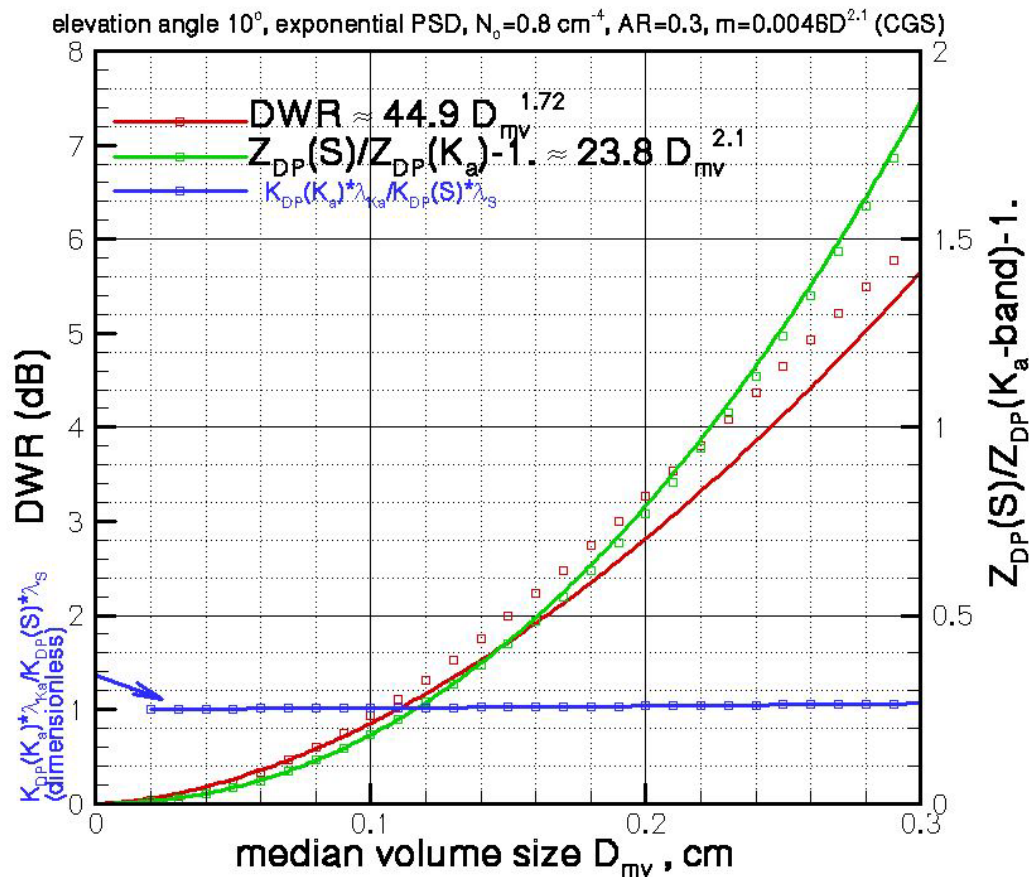
KASPR – Ka-band scanning polarimetric radar

KOKX WSR-88D S band

KASPR Ka band



Courtesy of
Sergey Matrosov



dwr-z-zdp-0.3-0.0046-2.1-s-ka.*

snow-dis-dwr-s-ka.for

- Polarimetric ice retrieval formulas are valid for Rayleigh scatterers and may not be applicable for snow at Ka band if $DWR \gg 0$ dB
- Because K_{DP} is affected only by Rayleigh-size particles in the spectrum, the product $K_{DP}\lambda$ is almost constant in a wide range of radar frequencies (Ka – S)
- There are two possible ways to make ice retrievals at Ka band
 - (1) Utilize $K_{DP}\lambda$ measured at Ka band and Z and Z_{DP} measured at longer wavelength or
 - (2) Use Matrosov's formulas to correct Z and Z_{DP} at Ka band

Estimation of the aspect ratio of ice particles

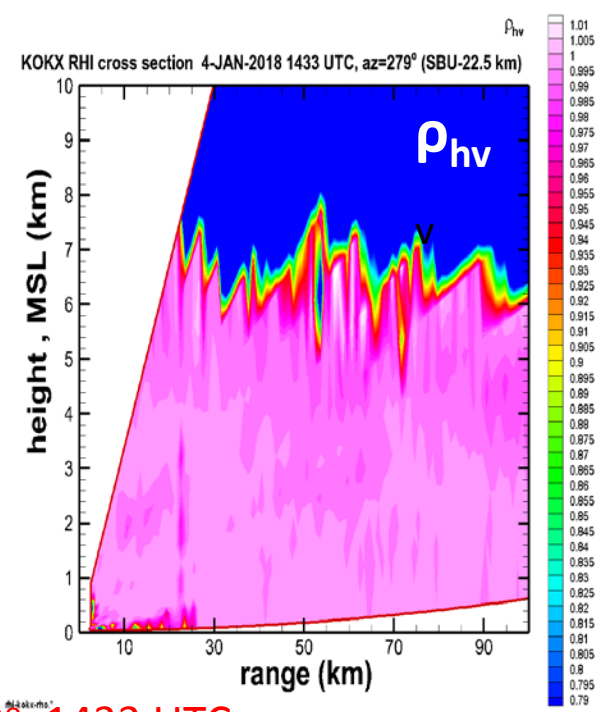
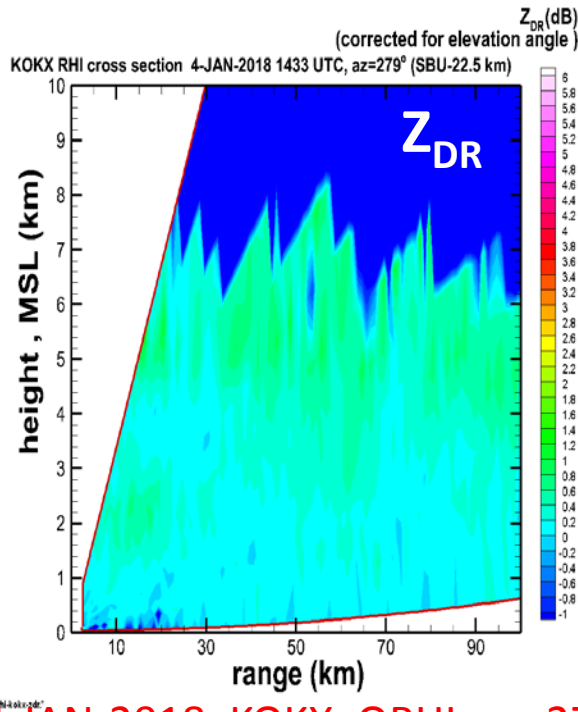
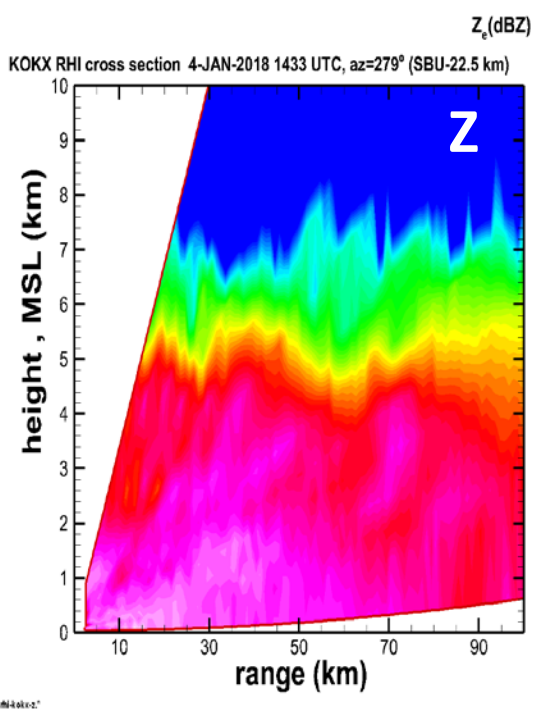
Matrosov et al. 2017

- As opposed to linear depolarization ratio (LDR), circular depolarization ratio (CDR) is weakly dependent on the particles' orientation and is mainly determined by their shape
- A CDR “proxy” can be obtained from the measurements in the linear (HV) polarimetric basis if LDR is available

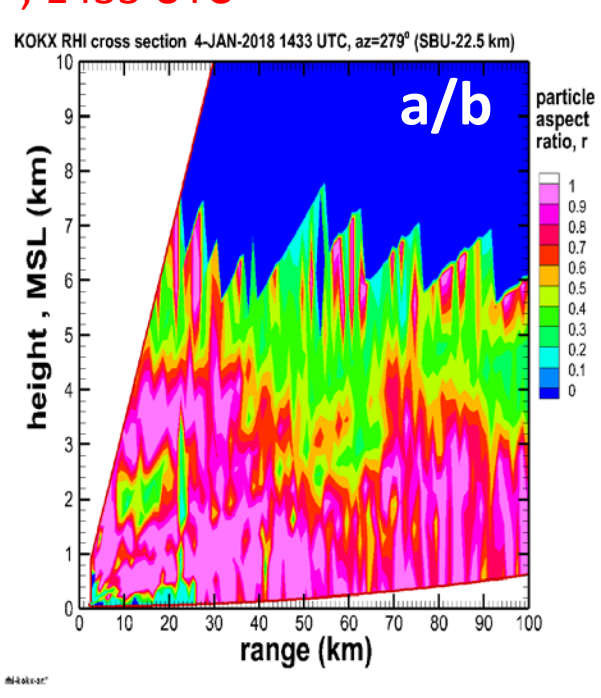
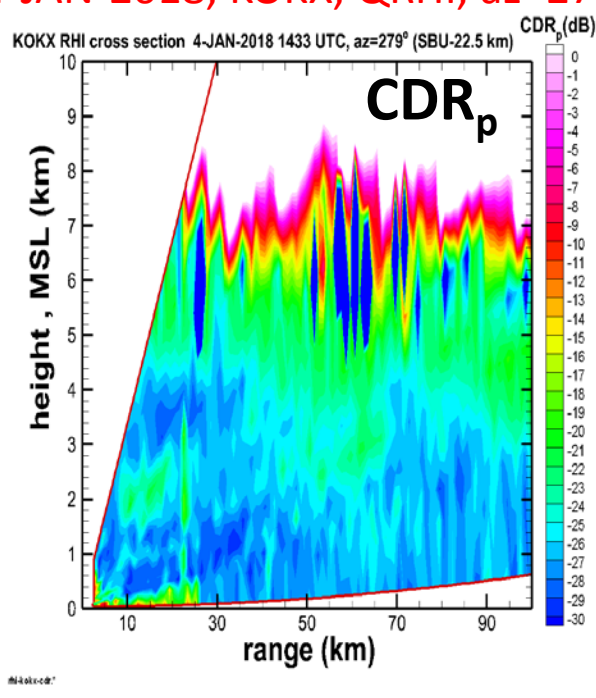
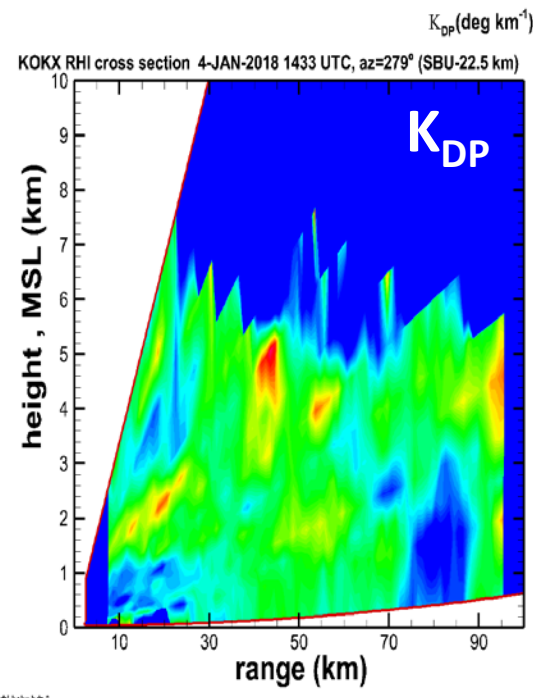
$$C'_{dr} = \frac{1 + Z_{dr} + 4Z_{dr}L_{dr} - 2\rho_{hv}Z_{dr}^{1/2}}{1 + Z_{dr} + 2\rho_{hv}Z_{dr}^{1/2}}$$

or from the measurements of Z_{DR} and ρ_{hv} by the standard polarimetric radars with simultaneous transmission / reception of H and V waves

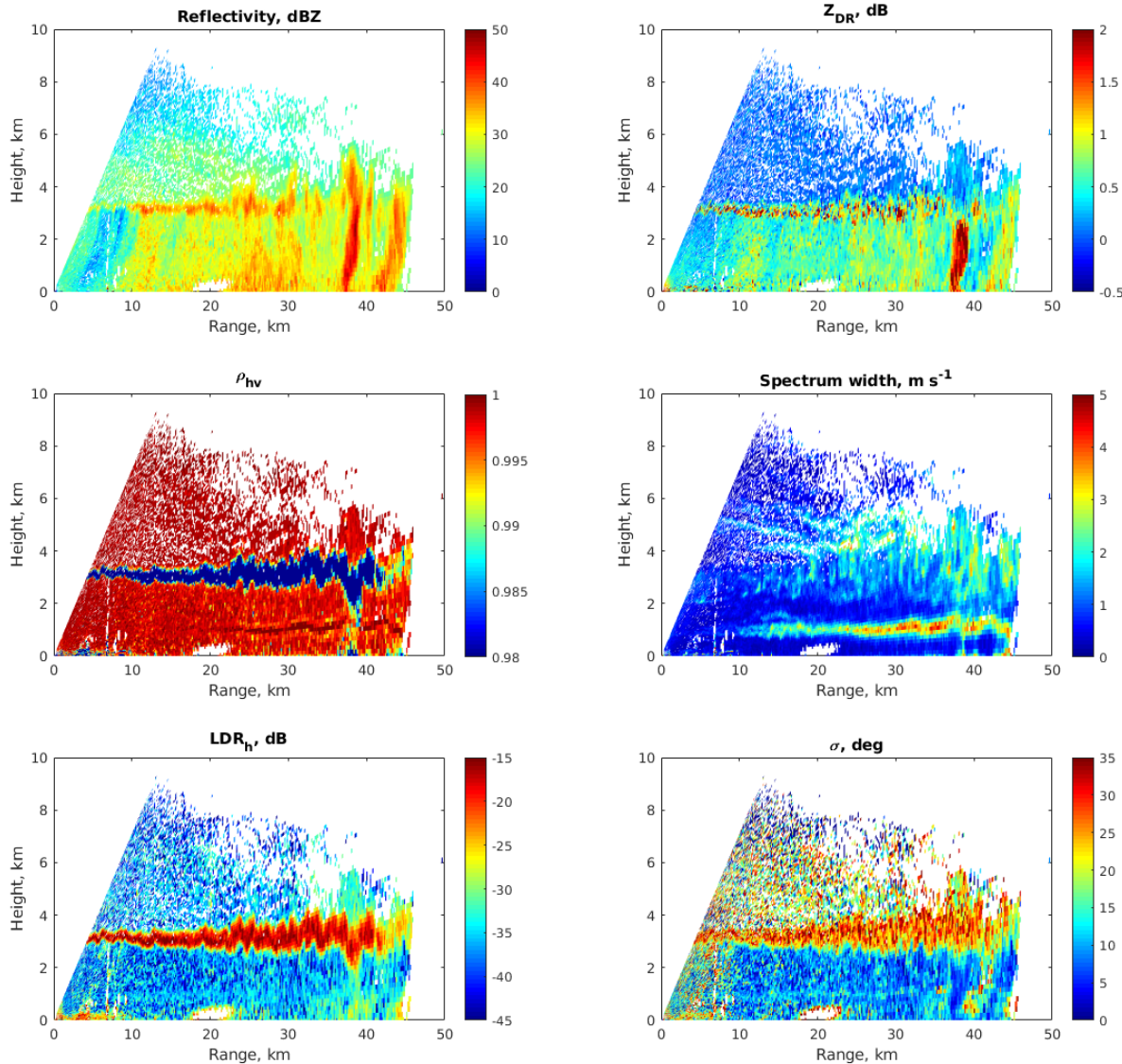
$$C''_{dr} = \frac{1 + Z_{dr} - 2\rho_{hv}Z_{dr}^{1/2}}{1 + Z_{dr} + 2\rho_{hv}Z_{dr}^{1/2}}$$



4-JAN-2018, KOKX, QRHI, az=279°, 1433 UTC



Estimation of the width of the canting angle distributions σ



NCAR S-Pol observations of nocturnal MCS (PECAN field campaign)

$$\sigma(\text{deg}) = \frac{180}{\pi} \frac{L_{dr}^{1/2}}{(1 + Z_{dr}^{-1} - 2\rho_{hv}Z_{dr}^{-1/2})^{1/2}}$$

Dry and wet snowflakes are more randomly oriented than raindrops

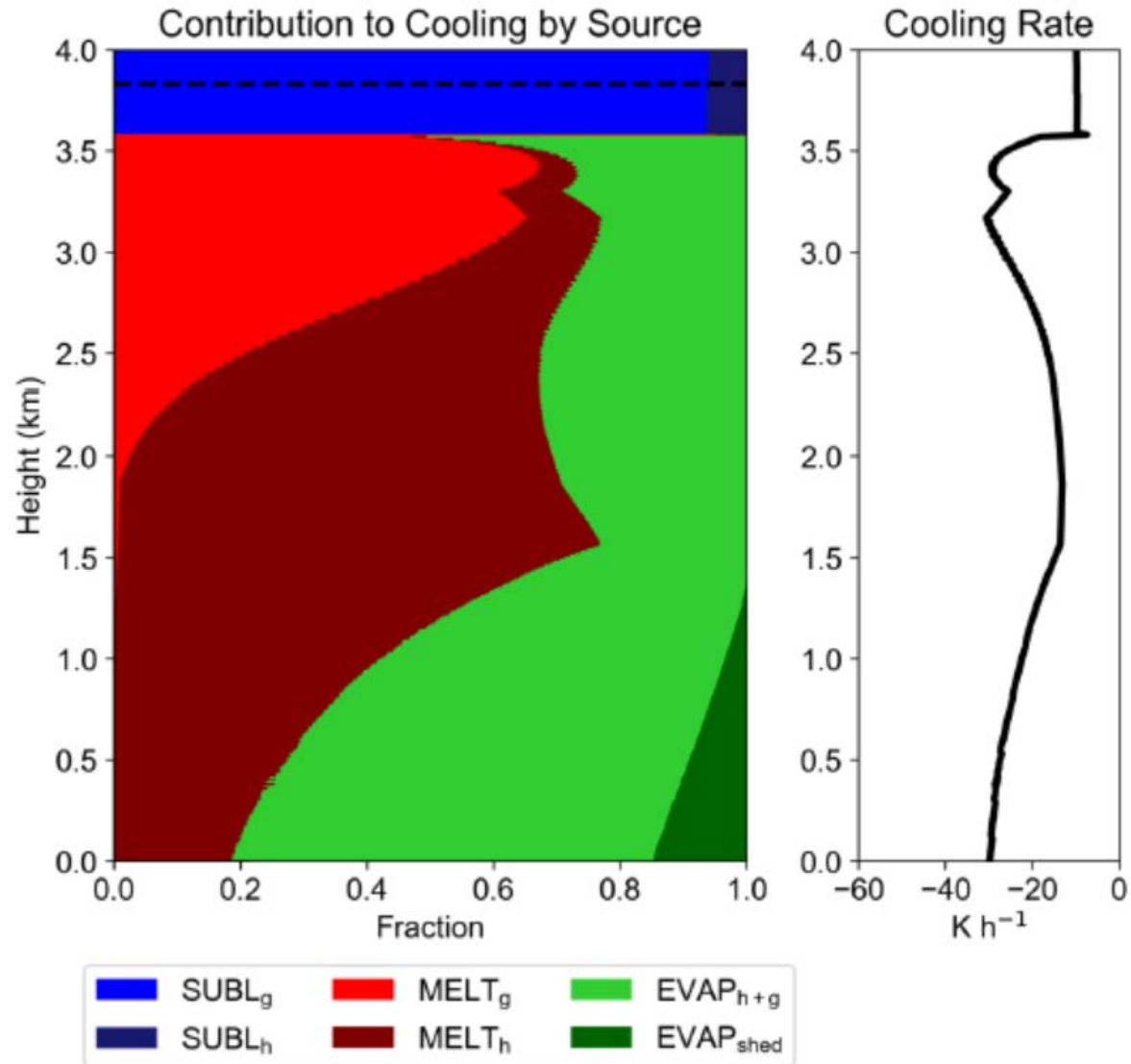
Thermodynamic retrievals

Two 1D Lagrangian cloud models with spectral bin microphysics coupled with polarimetric forward operator are used to provide guidance for thermodynamic radar retrievals :

- (1) Model for melting graupel / hail - Ryzhkov et al. 2013:
“Polarimetric radar characteristics of melting hail. Pt I:
Theoretical simulations using spectral microphysical modeling”
- (2) Model for melting snow – Carlin and Ryzhkov 2019: “Estimation
of melting layer cooling rate from dual-polarization radar:
Spectral bin model simulations”

The models are initiated with either assumed or polarimetrically retrieved size distribution of graupel / hail or snow at certain height level above the melting layer. They do not simulate genesis of ice.

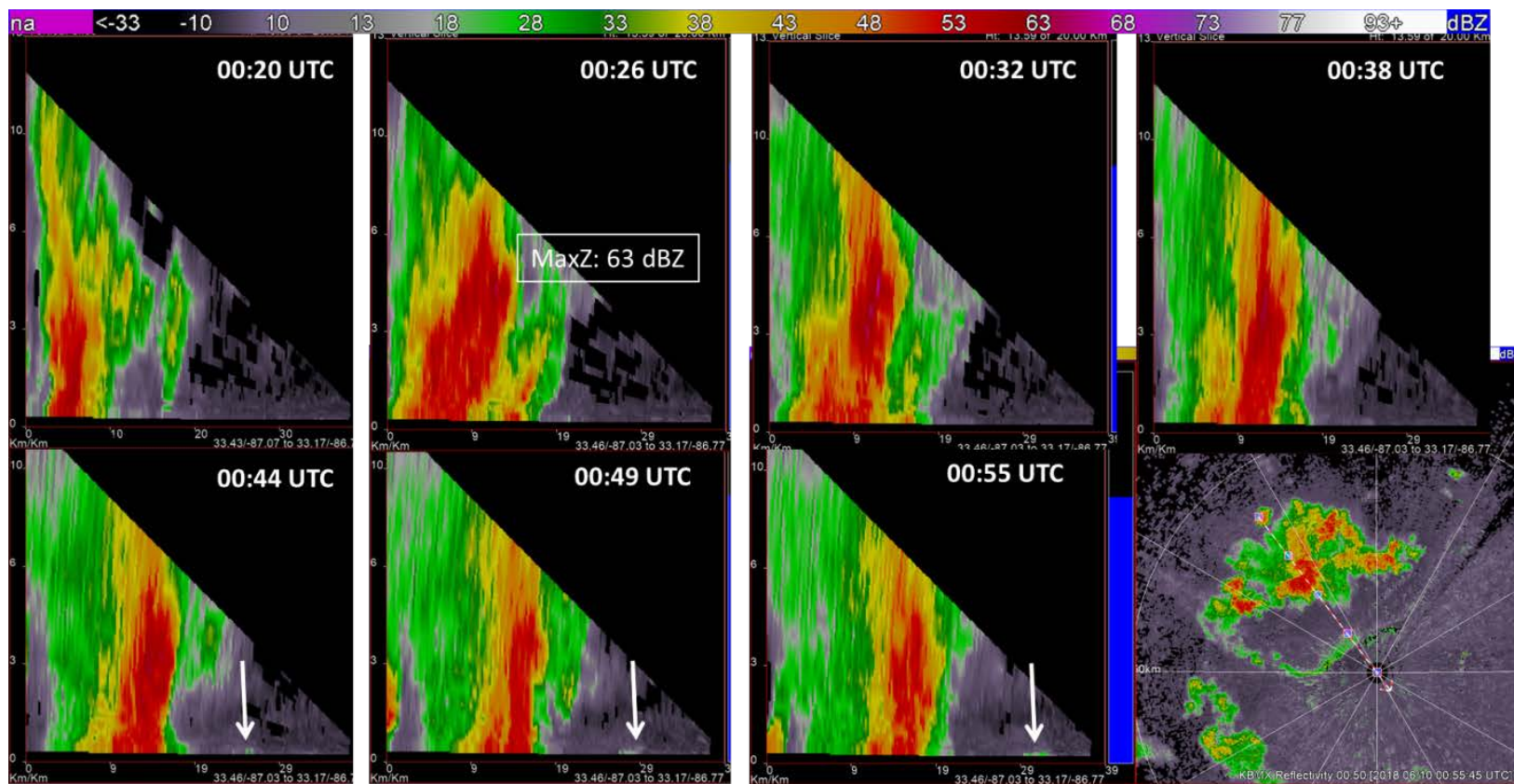
Contribution of different processes to cooling rates in hailstorms below the freezing level



Modeling and polarimetric detection of “cold pools” and microbursts

The microburst event in Alabama observed with the KBMX WSR-88D radar

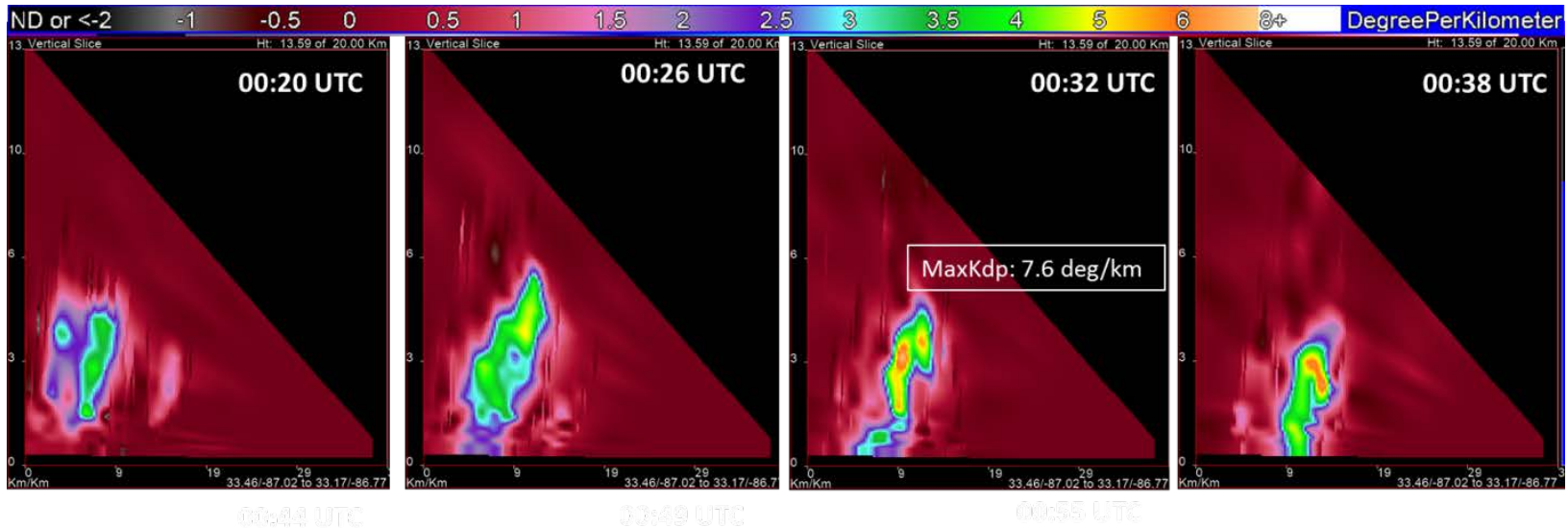
Descending reflectivity core



Modeling and polarimetric detection of “cold pools” and microbursts

The microburst event in Alabama observed with the KBMX WSR-88D radar

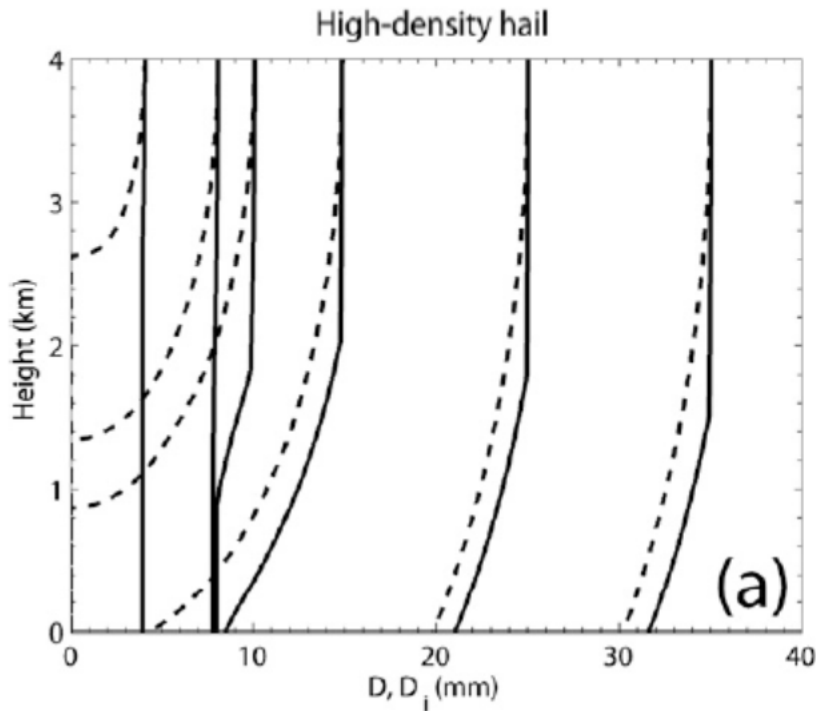
Descending K_{DP} core



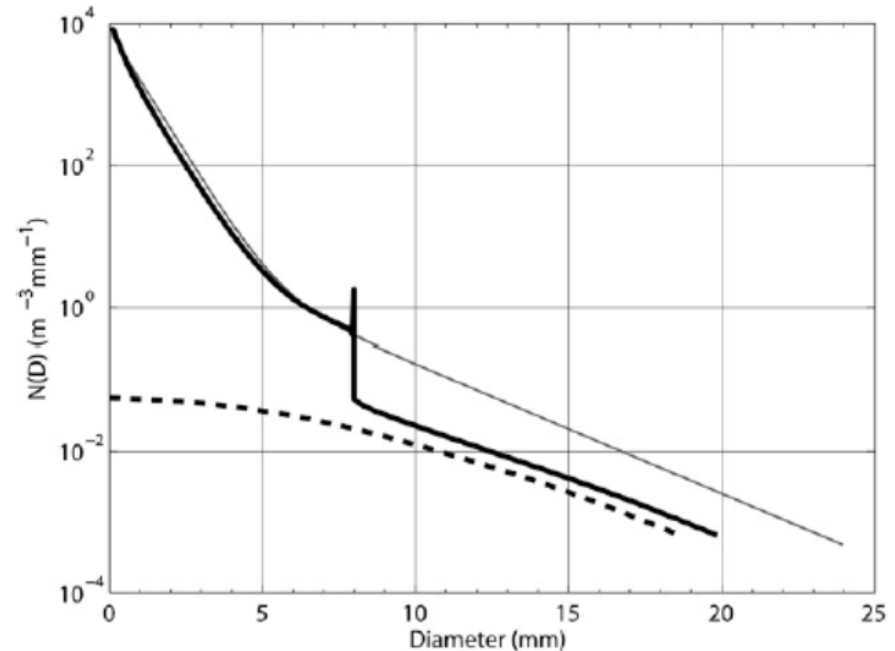
There is a strong evidence that descending K_{DP} columns with anomalously high K_{DP} are associated with high concentration of small hail and signal imminent microburst at the surface (Frugis et al. 2018; Kumjian et al. 2019)

$K_{DP} < 5$ deg/km in pure rain at S band whereas Kumjian et al. (2019) reported $K_{DP} > 17$ deg/km !

Ryzhkov et al. (2013) model of melting hail predicts strong enhancement of concentration of water coated hailstones with sizes 8 – 13 mm

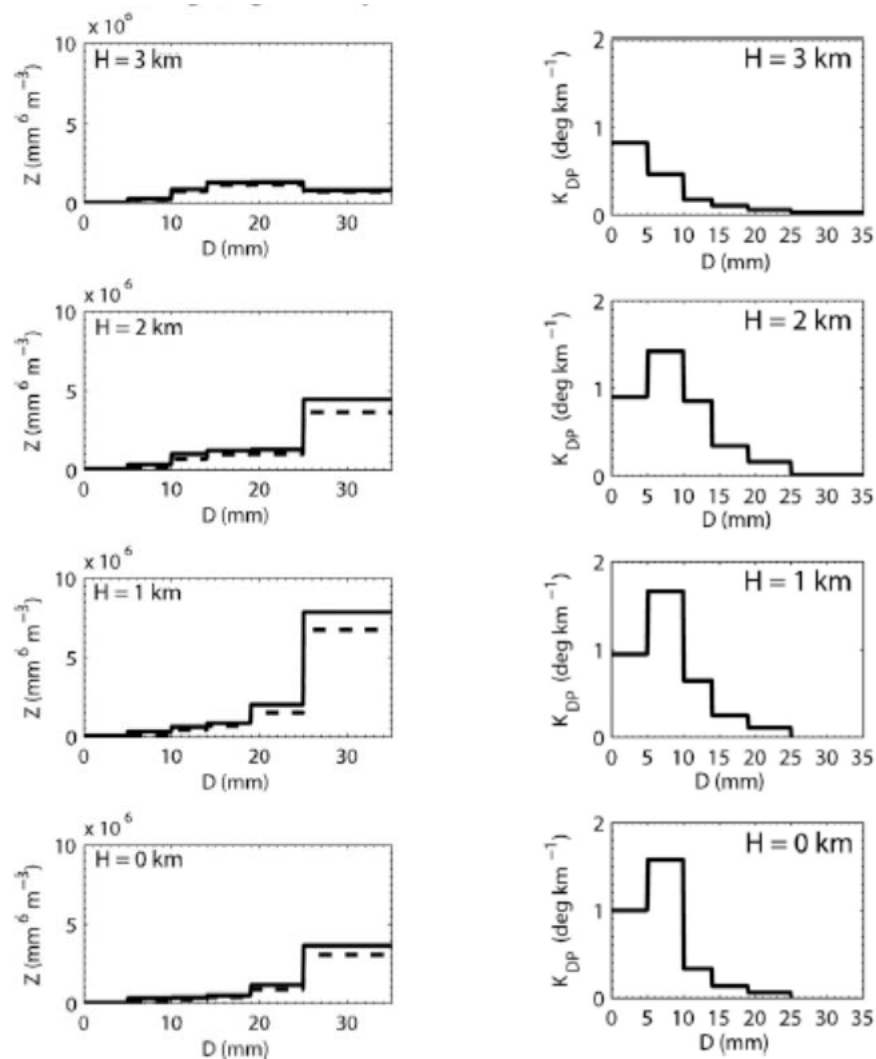


Diameters of melting hailstones (solid lines) and their ice cores (dashed lines) as functions of height below the freezing level



Size distributions of ice particles at $H = 4$ km (thin solid grey line), raindrops and melting hailstones at $H = 0$ km (thick solid line), and ice cores at $H = 0$ km (dashed line) for moderate hail.

Relative contributions of different parts of the particle size spectrum to S-band and C-band Z (left column) and S-band K_{DP} (right column) at different heights
Ryzhkov et al. (2013)



Z is primarily determined by large hail whereas K_{DP} – by small hail and raindrops

1D Lagrangian model of falling snow (Jacob Carlin)

Additions to 1-D Spectral Bin Model:

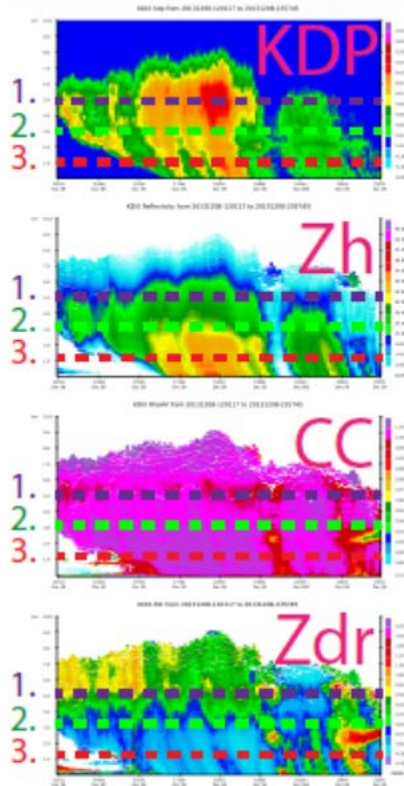
- Evaporation
- Depositional growth / sublimation
- Environmental feedback of latent heating/cooling and moistening/drying
- Explicit calculation of non-equilibrium particle temperature
- Modifications to polarimetric radar operator (e.g., mixed-phase dielectric factor, aspect ratio of aggregates)
- PSDs defined at model "top" (i.e., specify snow distributions → can be paired with retrievals from QVPs)
- Extended to pristine ice habits (dendrites, plates, needles)

Current Efforts:

- Aspect ratio evolution via "adaptive" growth for crystal habits (e.g., Chen and Lamb 1994; Harrington et al. 2013; Jensen et al. 2017)
- Explicit treatment of aggregation (and break-up?) with multiple concurrent habits

Aggregation of snow

Radar Observations

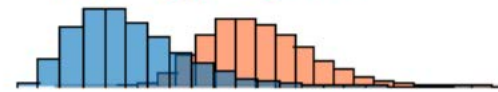


Possible Ice Particle Distributions

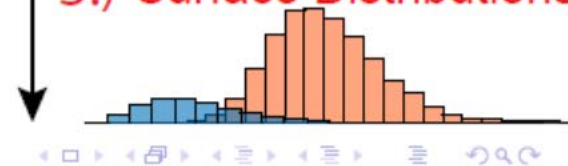
■ Plates/Dendrites?



2.) Aggregation

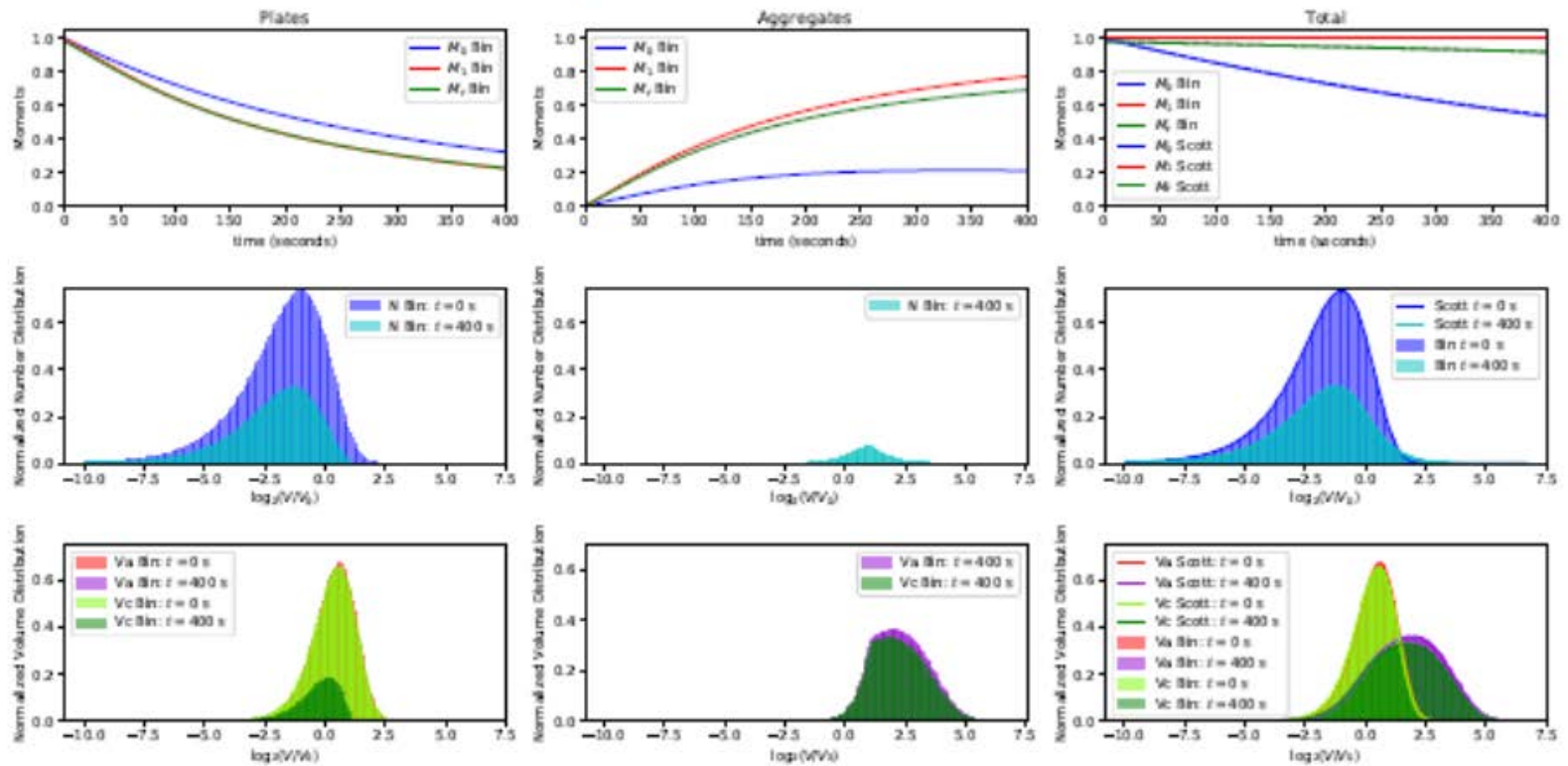


3.) Surface Distributions



Testing of the aggregation module (E. L. Dunnavan)

Preliminary Box Model Results

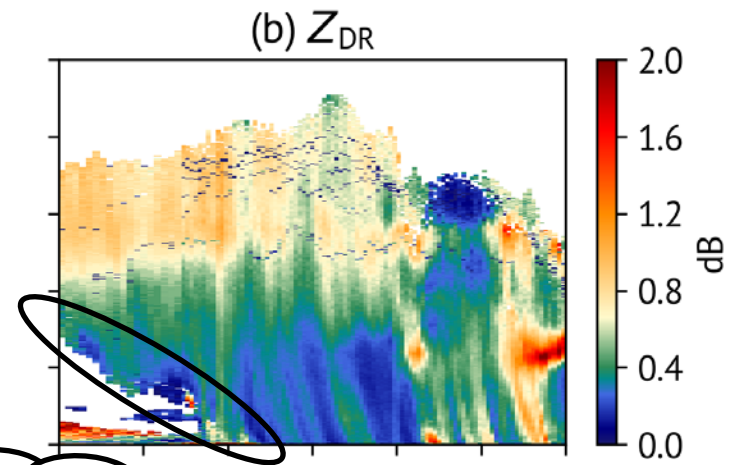
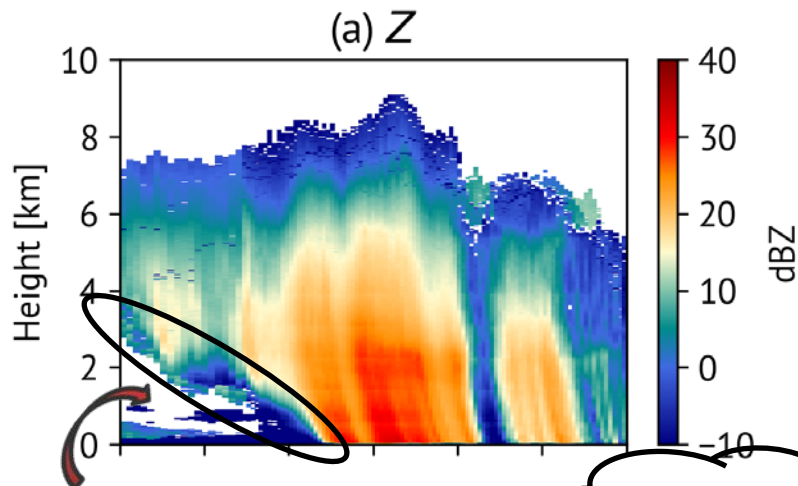


**“Snowbowl” surprise
snowstorm
Philadelphia, PA
08 December 2013**



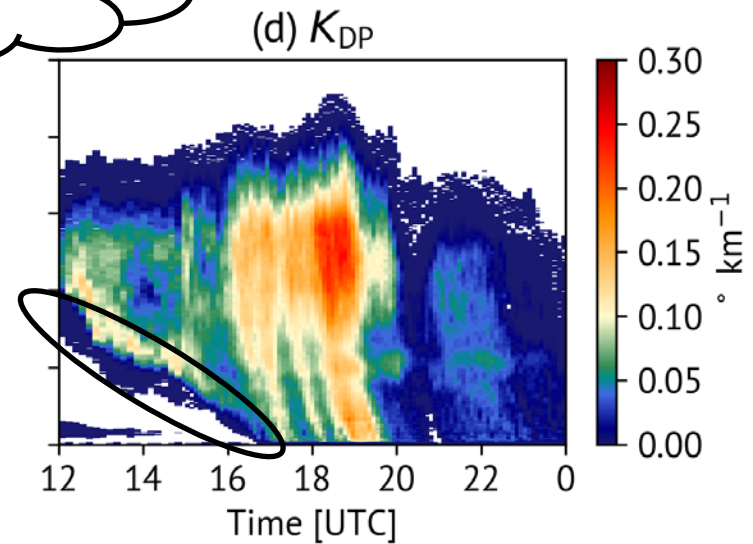
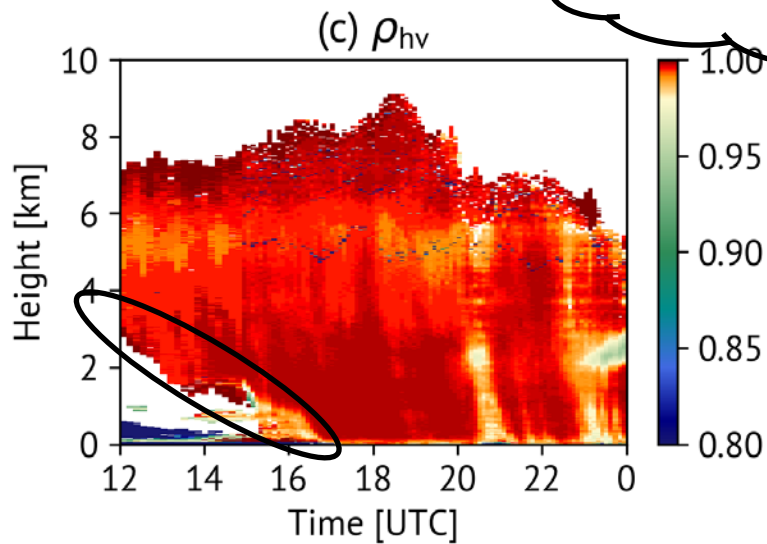
KDIX Range-defined Quasi-Vertical Profile (RDQVP; Tobin and Kumjian 2017) on 08 Dec 2013

(corrected for estimated -0.3125 dB bias)

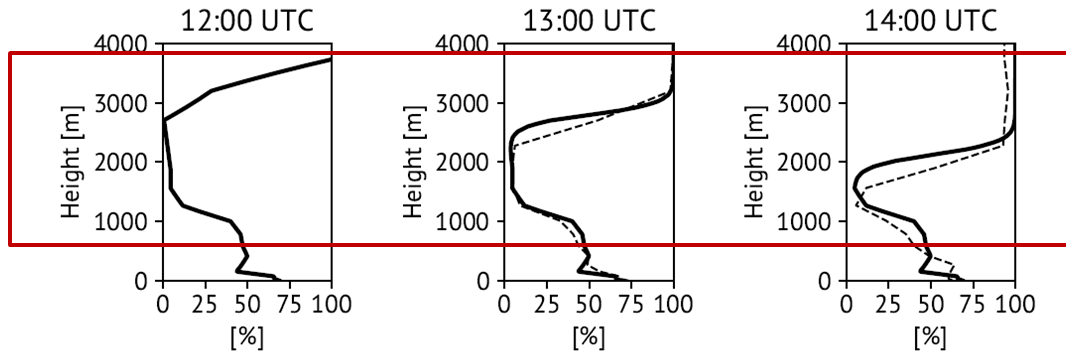


Dry layer with RH_i as low as 5%!

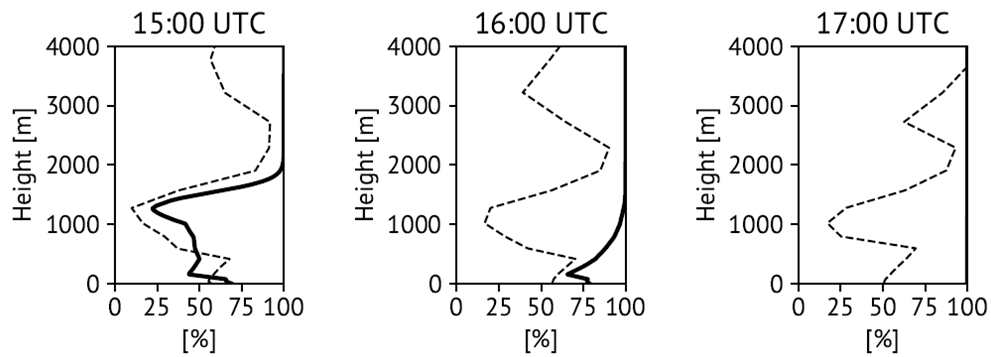
Strong Sublimation



Evolution of Vertical Profile of RH_i



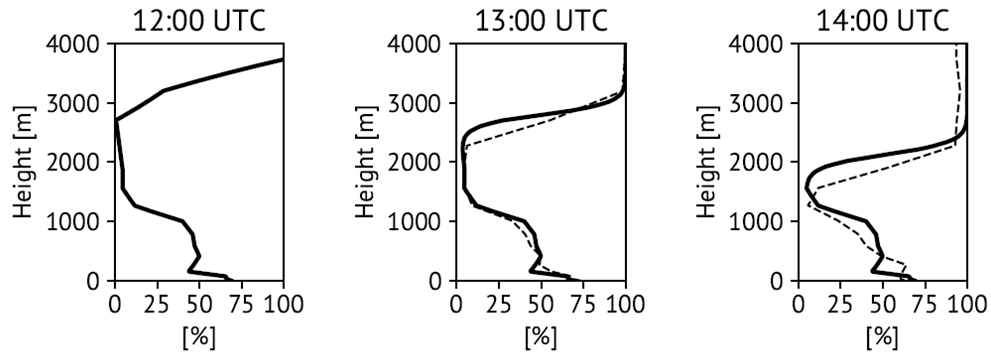
Good agreement of progression of moistening



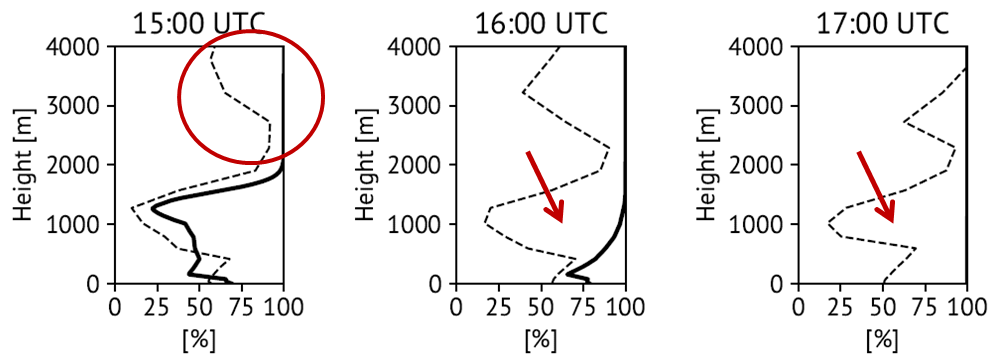
—— ID Model

----- RAP Analyses

Evolution of Vertical Profile of RH_i

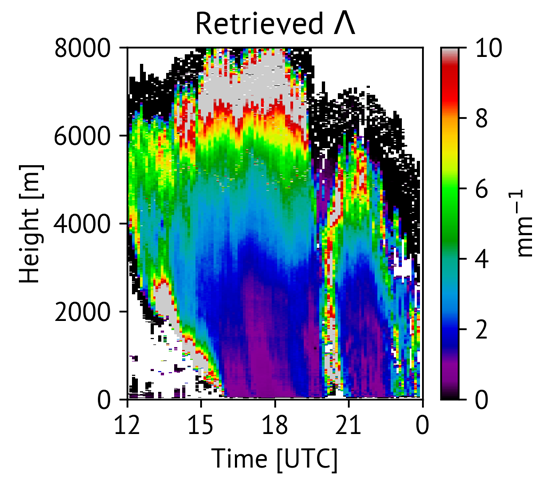
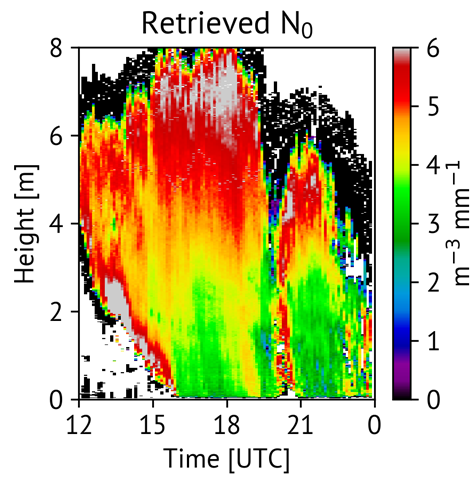


Erroneous dry air aloft prevents correct moistening of low levels

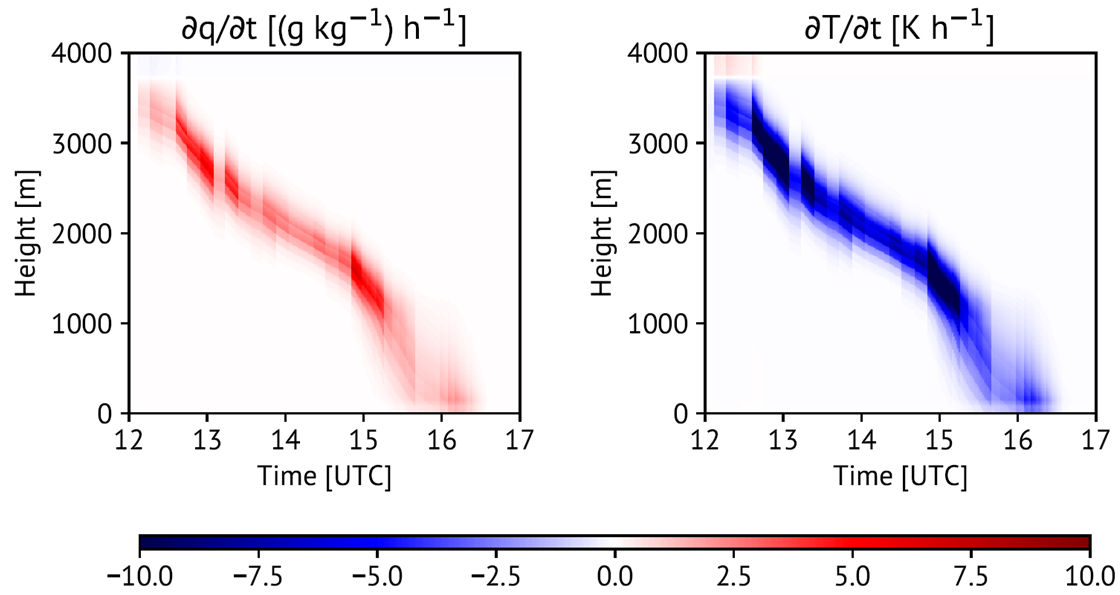


———— ID Model

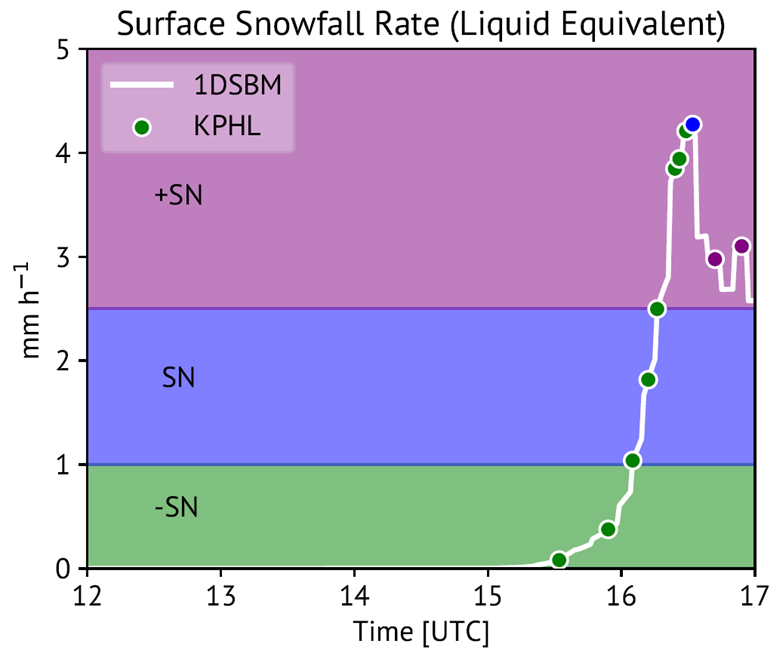
----- RAP Analyses



Initialized 1-D model with snow aggregates retrieved from RDQVP data and environmental data from RAP.



1-D model captures cooling and moistening progressing toward the surface.



1-D model successfully predicted start time of snow at surface and increase to heavy snow shortly thereafter (~30 min too early).